

**PROGRESS IN PREDICTING THE DECAY
OF SATELLITE AND DEBRIS ORBITS**

Kenneth Moe *
Space Environment Technologies

Abstract

We know the equations that govern the decay of a satellite orbit. Why then is it so difficult to make satisfactory orbital predictions? The reason is that several of the quantities in the equation are highly variable or poorly known: The air density depends on processes in the sun and in interplanetary space, as well as in our atmosphere; the drag coefficient varies with satellite shape, orientation, and altitude; and the velocity includes the orbital motion as well as the atmospheric wind, which can become enormous during geomagnetic storms. This paper describes recent progress in measuring and predicting these quantities.

Introduction

The in-track component of acceleration caused by air drag is related to the satellite characteristics through the fundamental relation

$$F_d = m a = \frac{1}{2} \rho V_i^2 C_d A_{ref} \quad (1)$$

where F_d is the in-track component of the force of air drag; a is the corresponding in-track component of acceleration; m is the mass of the satellite; ρ is the air density; C_d is the drag coefficient; A_{ref} is the reference area (usually taken to be the cross-sectional area of the satellite projected normal to the velocity vector); and V_i is the speed of the incident air molecules relative to the satellite. The values of the mass and the area are often known within 1 %, but the speed and drag coefficient are more uncertain. V_i is usually approximated by the orbital velocity (assuming that the atmosphere rotates with the earth). This generally causes negligible error, except at high latitudes during geomagnetic storms, where, for example, Feess¹ has measured winds that exceeded 1 km/sec. Winds of this magnitude can cause errors of 20 or 30 % in the density deduced from accelerometer measurements². If the satellite carries an accelerometer and a mass spectrometer or density gauge, one can solve for the in-track wind, thus removing this source of error^{3,4}. However, the uncertainties in the drag coefficient are important under all conditions of geomagnetic activity and at all latitudes and altitudes at which density is to be measured. In the past, a drag coefficient of 2.2 has often been assumed for all satellites of compact shapes. In this paper we report recent progress in measuring and calculating drag coefficients, and in measuring and predicting the other quantities that enter Equation (1),

* email address: kmmoe@att.net

Thermospheric Air Density, and Why it Varies

The Sun is the source of energy that maintains the upper atmosphere, but solar energy reaches the thermosphere through several different pathways: (1) Extreme ultraviolet radiation and X-radiation reach the Earth from the Sun in 8 minutes. They heat, ionize, and dissociate atmospheric gases. (2) Highly energetic particles from solar disturbances reach the earth in a few hours. (3) Ionized gases also escape through coronal holes, and create the Solar Wind, which reaches the vicinity of the Earth after several days of travel. The Solar Wind must penetrate the Earth's bow shock and magnetosphere before it can interact with our atmosphere. Figure (1) shows Willard Olson's model of the magnetosphere⁵. Plasma continuously flows through the dayside cusps of the magnetosphere to heat the high-latitude thermosphere⁵ and ionosphere⁶. Early efforts to incorporate cusp heating effects in thermospheric models^{7,8} were not adopted by other modelers. Now that the CHAMP/STAR accelerometer has confirmed continuous cusp heating⁹⁻¹¹, this energy source will likely be added to the commonly-used thermospheric models.

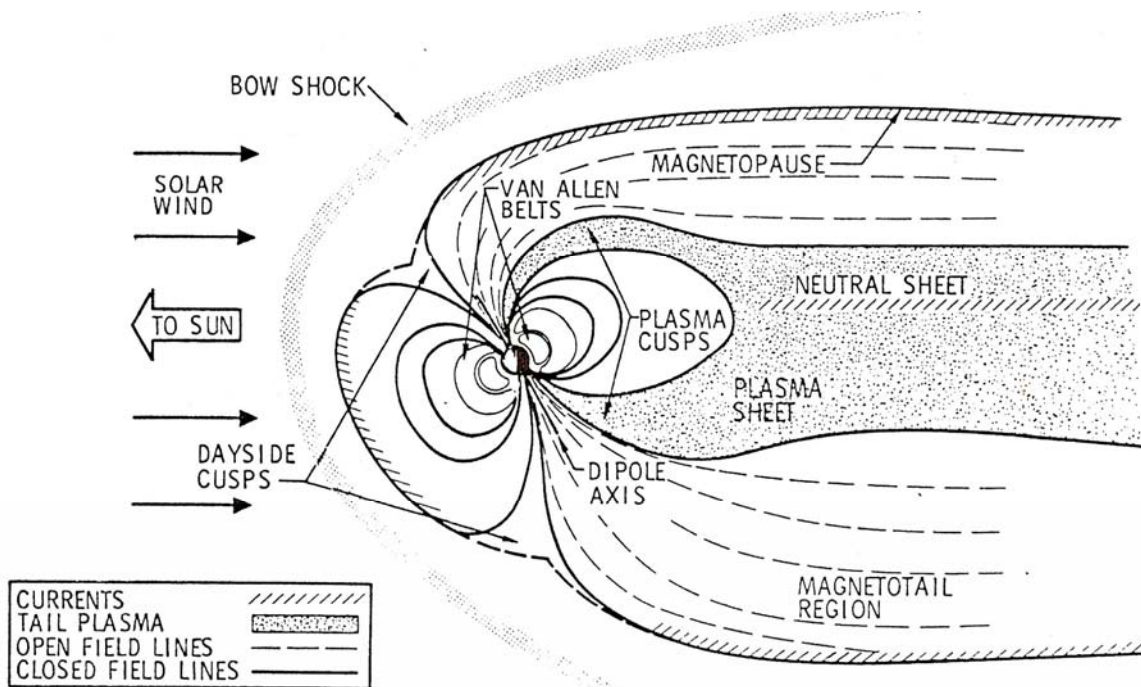


Fig.1. Willard Olson's model of the magnetosphere in the noon-midnight meridian. The Earth is the small sphere at the center. Shocked solar wind plasma flows continuously down the dayside cusps to heat the dayside auroral thermosphere. Geomagnetic storms occur sporadically when particles precipitate into the high latitude thermosphere from both open and closed field lines in the tail of the magnetosphere.

Sometimes, enormous solar eruptions greatly enhance the solar wind. If these enhanced streams reach the earth, they can overload the magnetosphere and produce geomagnetic storms. The increased energy input to the auroral zone reverses the normal wind pattern in the thermosphere^{12,13}. Tim Fuller-Rowell's general circulation model of the

thermosphere is able to calculate this change in wind patterns¹⁴. The largest geomagnetic storms can double or triple the thermospheric air density in a few hours, and last for a day or two^{15,16}. When the solar ultraviolet (UV) radiation increases, it can also double or triple the air density, but UV changes develop over a week or two¹⁷. UV radiation causes even larger density variations that gradually rise and then fall during an 11-year sunspot cycle¹⁸.

Early in the space age, many models were developed for calculating the density of the neutral thermosphere. The early development of models and measurements has been reviewed¹⁹. The AIAA maintains a report that documents thermospheric models²⁰. Two of these models, Jacchia, 1970, and MSIS, are still in operational use and have been revised frequently. Recently, Kent Tobiska has been improving the representation of the ultraviolet energy source²¹. Bruce Bowman has improved the semiannual variation in the Jacchia model²². Bowman and Tobiska²³ have recently used tracking data from many spherical and nearly spherical satellites to evaluate the result of these improvements in the Jacchia model. Modifying the energy source and the semiannual variation halved the discrepancies between model and tracking data. This evaluation was conducted on days when the geomagnetic planetary amplitude, A_p , was less than 25. Thermospheric models perform poorly during geomagnetic storms, when the solar wind overloads the magnetosphere and A_p can greatly exceed 25.

Winds during Geomagnetic Storms

When accelerometer measurements of density are analyzed, it usually is assumed that the only wind striking the spacecraft is caused by the rotation of the Earth. Most of the time, this is a good approximation. But at high latitudes during geomagnetic storms, this assumption can cause an error of several tens of percent in the deduced density¹⁻⁴. This is illustrated in the following composite figure: Figure 2a shows the densities measured by Philbrick, et al.²⁴ on the S3-1 satellite during a series of geomagnetic storms. The densities labeled Acc were measured at perigee by an accelerometer, assuming a drag coefficient of 2.2. The densities labeled MS were measured by a mass spectrometer on the same satellite. Notice that the densities measured by the two instruments frequently crossed each other: These crossings occurred during geomagnetic storms, when the densities and winds were high. The accelerometer measurement is proportional to the square of the velocity, while the mass spectrometric measurement is linearly related to the velocity. By solving the appropriate equations simultaneously, the in-track wind can be calculated^{2,4}. That calculation also makes it possible to compute the corrected densities shown in Figure 2b.

The corrected densities in Figure 2b move more nearly parallel, without the crossings that occur in Figure 2a. The remaining differences between the two instruments are caused by an incorrect drag coefficient, possible errors in calibrating the mass spectrometer, and random errors of measurement. Corrected drag coefficients have recently been calculated for the spinning S3-1 satellite⁴, so absolute densities can now be deduced from its accelerometer data.

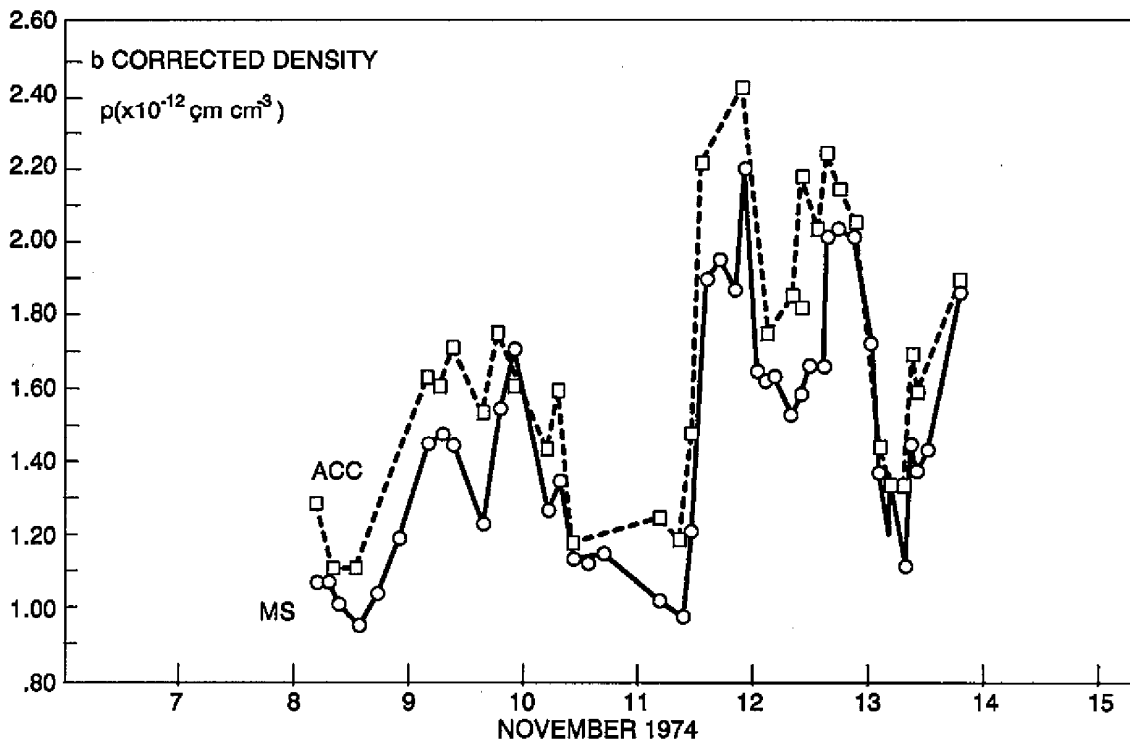
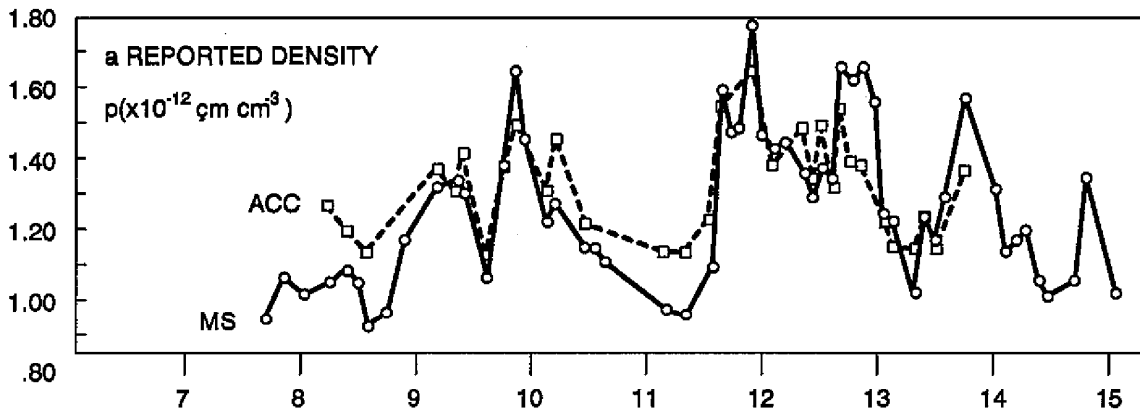


Fig.2. Density measurements from the S3-1 accelerometer (Acc) and mass spectrometer (MS) as originally reported by Philbrick, et al. are shown in panel a. Panel b shows the same measurements corrected for winds, using the technique described in the text and references.

In recent years, the STAR accelerometer is being flown on the CHAMP Satellite. Bruinsma et al.¹⁰ and Liu, et al.¹¹ have deduced densities from its accelerometer measurements, but have omitted the data during geomagnetic storms because of uncertainty about the winds. Because the ionosphere is a minor constituent embedded in the neutral thermosphere, the winds can be calculated from data archived by the ionosonde network¹³. A simultaneous analysis of data collected by the accelerometer

and the ionosondes could then calculate thermospheric densities during geomagnetic storms.

Drag Coefficients

When thermospheric densities are deduced from accelerometer measurements, or from satellite orbital decay, a drag coefficient must be supplied by the analyst, because the drag coefficient is not measured in the experiment. In the past, the value 2.2 has often been used for compactly shaped satellites, and values above 3 for long cylindrical satellites that fly like an arrow²⁵. Sufficient orbital measurements of gas-surface interactions have now accumulated that we can calculate drag coefficients of satellites in low-earth orbit up to 325 km with considerable confidence²⁶. These are shown for four compact shapes in Figure 3.

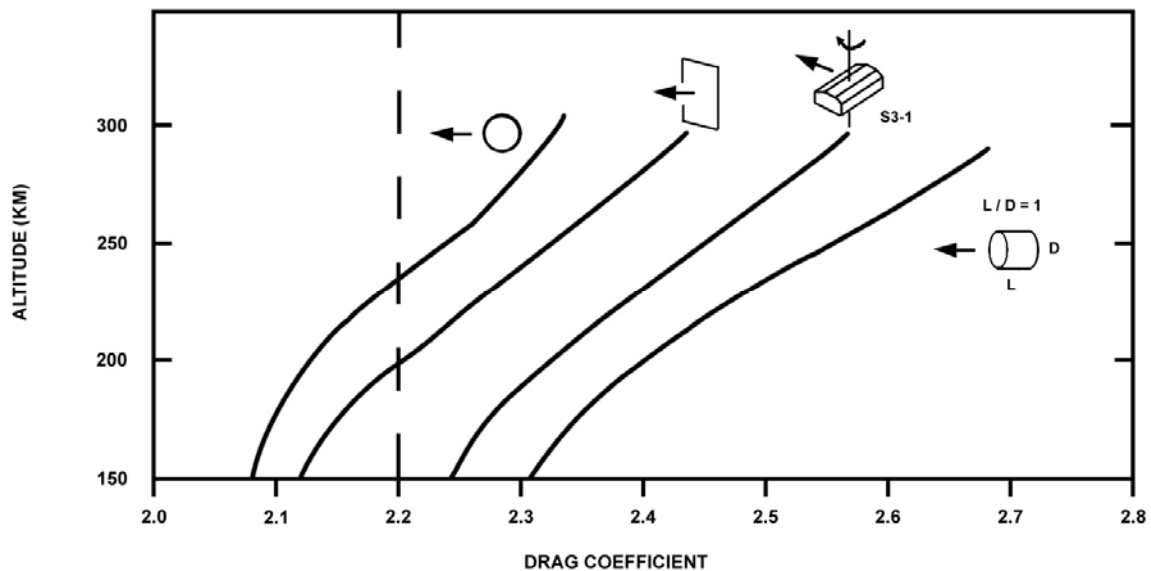


Fig.3. Drag coefficients in LEO for a sphere, a flat plate at normal incidence, the spinning S3-1 Satellite, and a short cylinder with a flat plate in front. These curves have been calculated assuming completely diffuse reemission, using parameters of gas-surface interaction measured in orbit at times of low solar activity. The widely used value of 2.2 is shown dashed for comparison.

Above 300 km, the uncertainty in these calculations increases rapidly, because an increasing fraction of the incident molecules can be reemitted quasi-specularly. This uncertainty is shown for the sphere and short cylinder by the shaded areas in Figure 4. I have been working with Bruce Bowman of the Air Force Space Command to reduce the uncertainties in drag coefficients above 300 km²⁷, and to measure the effect of satellite surface material on the drag coefficient.²⁸ It is important to extend this work because drag coefficients will play a key role in efforts to improve thermospheric models and validate the new Air Force programs that monitor and predict thermospheric density.^{27,29}

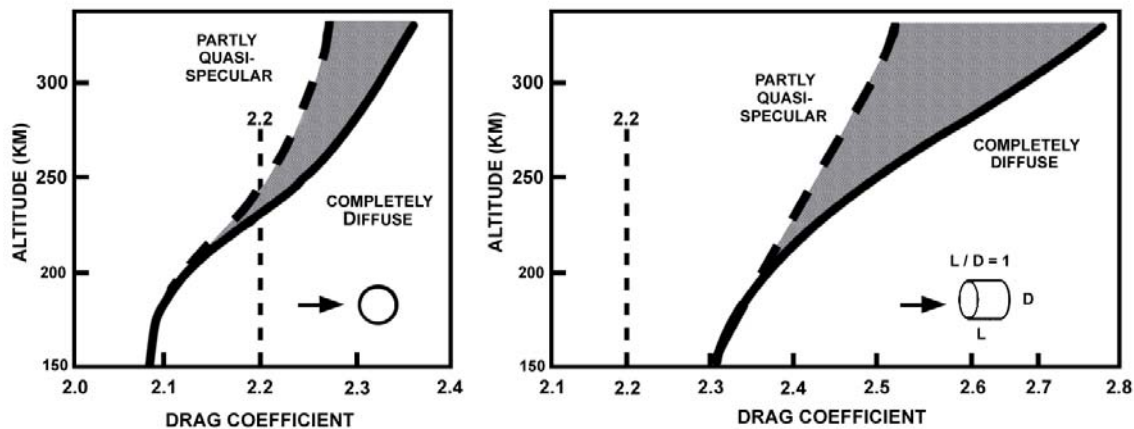


Fig. 4. Uncertainties in drag coefficients caused by quasi-specular reemission at the higher altitudes. The solid curves assume completely diffuse reemission. The dashed curves represent our estimated upper bound on the quasi-specular reduction of the drag coefficients.

(NOTE: A drag coefficient used in orbit fitting should not be confused with a (physical) drag coefficient used in measuring density. Orbit analysts often adjust the drag coefficient to make the tracking data fit a model. The nominal density from the model is not the actual density, nor is the fitted drag coefficient the true (physical) drag coefficient.)

Atmospheric Monitoring

In recent years, the Air Force has used a two-pronged approach in its efforts to improve the monitoring of thermospheric density.^{27,29} One approach, which was pioneered in Russia by L. L. Volkov and V. V. Yastrebov³⁰, and brought to the United States by Andrey Nazarenko and Vasiliy Yurasov^{31,32} consists in adjusting a density model to agree with the average orbital decay of many satellites in real time. The second method, which was suggested by the Naval Research Laboratory, consists in installing Ultraviolet Spectrometers on DMSP satellites, and using spectroscopic observations to monitor the air density²⁹. The fundamental spectroscopic parameters were shown by Torr, et al. to agree with composition (hence density) measurements within a factor of two in the definitive Atlas-1 experiment³³, so it has been difficult to achieve the 10 % accuracy required by the Joint Requirements Oversight Council (JROC).³⁴ Data from the Global Ultraviolet Imager (GUVI) on the TIMED Satellite now are being used to develop and evaluate methods of using spectroscopic sensors on DMSP Satellites.²⁹

As was mentioned in the section on Atmospheric Density, recent improvements in the Jacchia model made by Bowman and Tobiska²³ have reduced the discrepancies between the model and orbital decay data by 50 %: The numerical values were 16 % rms errors before correction and 8 % after correction. The spectroscopic data are more difficult to evaluate, but Frank Marcos²⁹ has allowed for the differences in the nature of the measurements by taking ratios of the GRACE accelerometer densities to the MSIS thermospheric model, and the ratios of GUVI spectrometric measurements to the MSIS

model. He then took the double ratio, to compare the accelerometer with the spectrometer. Marcos found that the ratio of densities ranged from 0.6 to 1.6 during the year 2002. The double ratio is plotted as a function of latitude and date in Figure 5.

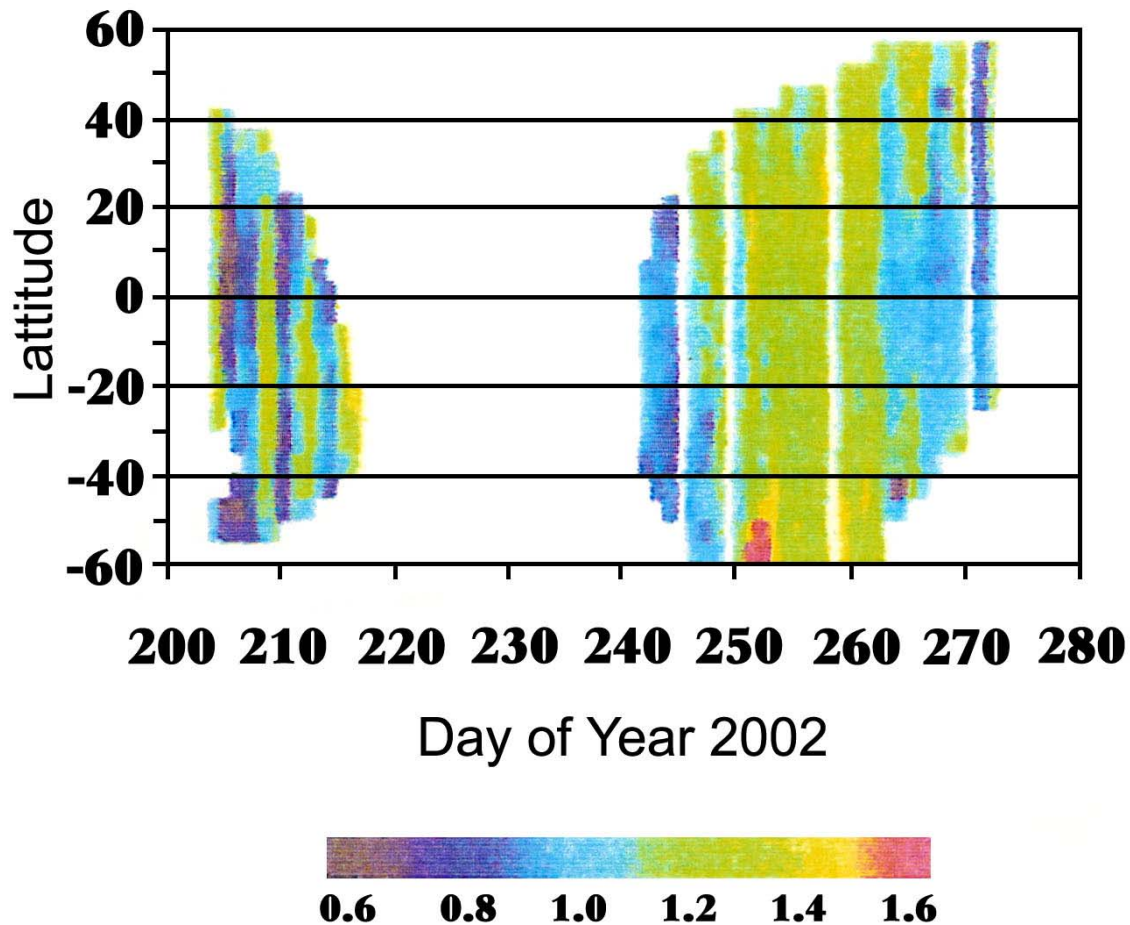


Fig. 5. Ratios of Grace accelerometer density measurements to GUVI spectroscopic density measurements, after Frank Marcos. The ratio in late 2002 ranged from 0.6 to 1.6 at altitudes near 350 km.

Orbital Debris

Near-Earth space has become relatively crowded with old satellites and their fragments. This has led to international efforts to improve space traffic management³⁵, and to utilize nanotechnology to measure spacecraft breakup during reentry³⁶. Electrodynamics tethers to deorbit debris have been studied³⁷. Models have been developed that predict the dispersal and orbital decay of spacecraft fragments³⁸, and the collision of spacecraft with debris³⁹. Eleven space agencies are involved in the Inter-Agency Space Debris Coordination Committee (IADC), which is coordinating international efforts to understand and mitigate the hazards caused by debris.

Efforts to Predict Air Density from Solar Activity

Motion pictures of the optical surface of the sun reveal a seething mass of plasma, from which streams of ions and electrons are continually escaping to produce the solar wind. Electric and magnetic field lines are attached to these ionized streams, so interplanetary space contains a complicated, ever-changing electromagnetic field. As new ionized streams emerge from the sun, they are diverted from a smooth path by the fields already present. This makes it difficult to predict the path of the solar wind, even when we monitor the solar emissions. NASA is planning to improve the monitoring of the solar-terrestrial environment by flying the Solar Dynamics Observatory in 2008.

Judith Lean⁴⁰ has recently published an informative paper about the solar emissions and their effects on the earth's atmosphere. Extensive research programs are underway to understand the physical processes in the sun and in interplanetary space⁴¹⁻⁴³. A group of scientists is working to evaluate real-time predictions of the time it takes solar eruptions to reach the Earth through the solar wind⁴⁴⁻⁴⁶.

Summary

This paper has summarized the present state of knowledge of the parameters needed to measure thermospheric densities and make orbital predictions: Densities, drag coefficients, winds, solar activity, and density models. Methods of improving present knowledge have been suggested.

References

1. Feess, W. A., 1973. Logacs wind analysis, in The Low-G Accelerometer Calibration System, Vol. II, TR 0074(4260-10) -1, Aerospace Corp., El Segundo, CA, 7-1 to 7-39.
2. Moe, K., and Moe, M. M., 1992. Deduction of in-track winds from satellite measurements of density and composition, *Geophys. Res. Lett.*, 19, 1343-1346.
3. Moe, K., and Moe, M. M., 1992. Correction of density and composition measurements for perturbations caused by in-track winds, AGU Chapman Conf. on the Upper Mesosphere and Lower Thermosphere, POSTER Session 8, Paper 14.
4. Moe, K., Rice, C.J., and Moe, M. M., 2004. Simultaneous analysis of multi-instrument satellite measurements of atmospheric density. *J. Spacecraft and Rockets*, 41, 849-853.
5. Olson, W. P., and Moe, K., 1974. Influence of precipitating charged particles on the high-latitude thermosphere, *J. Atmos. Terr. Physics*, 36, 1715-1726.
6. Titheridge, J. E., 1976. Ionospheric heating beneath the magnetospheric cleft, *J. Geophys. Res.*, 81, 3221-3226.
7. Moe, K., Olson, W. P., Moe, M., and Oelker, G., 1975. A thermospheric model which includes magnetospheric, tropospheric, and ultraviolet energy sources, EOS, *Trans. of the Am. Geophys. U.*, 56, 626-628.
8. Moe, K., and Moe, M. M., 1975. A dynamic model of the neutral thermosphere, a rept. to AFOSR on contract F44620-72-C-0084, McDonnell-Douglas Astronautics Co., Huntington Beach, CA.

9. Luehr, H., Rother, M., Koehler, W., Ritter, P. and Grunwaldt, L., 2004. Thermospheric up-welling in the cusp region: Evidence from CHAMP observations, *Geophys. Res. Lett.*, 31, L06805.
10. Bruinsma, S., Tamagnan, D., and Biancale, R., 2004. Atmospheric densities derived from CHAMP/STAR accelerometer observations, *Planet. Space Sci.*, 52, 297-312.
11. Liu, H., Luehr, H., Henize, V., and Koehler, W., 2005. Global distribution of the thermospheric total mass density derived from CHAMP, *J. Geophys. Res.*, 110, A04301.
12. Cole, K. D., 1962. Joule heating of the upper atmosphere, *Australian J. Phys.*, 15, 223.
13. Obayashi, T., and Matuura, N., 1972. Theoretical model of F-region storms in the upper atmosphere, Part 4, in *Solar-Terrestrial Physics*, edited by S. A. Bowhill, D. Riedel Publ. Co., Dordrecht, 199.
14. Fuller-Rowell, T. J., Codrescu, M. V., Moffett, R. J., and Quegan, S., 1994. Response of the thermosphere and ionosphere to geomagnetic storms, *J. Geophys. Res.*, 99, 3891-3914.
15. Bruce, R. W., 1973. Upper atmospheric density determination from LOGACS, in *The Low-G Accelerometer Calibration System*, Vol. II, Rept. No. TR-0074 (4260-10), Vol. II. Aerospace Corp., El Segundo, CA, pp. 1-1 to 1-43.
16. DeVries, L. L., 1972. Structure and motion of the thermosphere, in *Space Research XII*, Akademie-Verlag, Berlin (GDR), Vol. b, p. 867.
17. Priestler, W., 1965. Presentation to the Royal Society comparing density measurements with a model, *Proc. Roy. Soc. A*, 288, 493-509.
18. NOAA, NASA, and USAF, 1976. *US Standard Atmosphere*, 1976.
19. Moe, K., A review of atmospheric models in the altitude range 100 to 1000 km, 1969. AIAA Paper 69-50, AIAA, Reston, Virginia.
20. AIAA Guide to Reference and Standard Atmosphere Models, 2004. (G003B-2004) AIAA, Reston, Virginia.
21. Tobiska, W. K., 2005. Advances in solar inputs for precision orbit determination, AAS Paper 05-252, AAS Publications Office, PO Box 28130, San Diego, CA 92198.
22. Bowman, B. R., 2004. The Semiannual Thermospheric Density Variation From 1970 to 2002 Between 200-1100 km, AAS Paper 2004-174, AAS Publications Office, PO Box 28130, San Diego, CA 92198.
23. Bowman, B. R., and Tobiska, W. K., 2006. Improvements in modeling thermospheric densities using new EUV and FUV solar indices, AAS Paper 06-237, AAS Publications Office, PO Box 28130, San Diego, CA 92198.
24. Philbrick, C. R., McIsaac, J. P., and Faucher, G. A., 1977. Variations in atmospheric composition and density during a geomagnetic storm, *Space Research XVII*, edited by M. J. Rycroft and A. X. Strickland, Pergamon, Oxford, 349-353.
25. Moe, K., Moe, M. M., and Wallace, S. D., 1998. Improved satellite drag coefficient calculations from orbital measurements of energy accommodation. *J. Spacecraft and Rockets*, 35, 266-272.
26. Moe, K. and Moe, M. M., 2005. Gas-surface interactions and satellite drag coefficients, *Planet. Space Sci.*, 53, 793-801.
27. Bowman, B. R., and Moe, K., 2005. Drag coefficient variability at 175-500km from the orbit decay analyses of spheres, AAS 2005-257, AAS Publications Office, PO Box 28130, San Diego, CA 92198.

28. Moe, K., and Bowman, B.R., 2005. The Effects of Surface Composition and Treatment on Drag Coefficients of Spherical Satellites, AAS 2005-258, AAS Publications Office, PO Box 28130, San Diego, CA 92198.
29. Marcos, F. A., 2005. New measurements of thermospheric neutral density: A review, AAS 05-251, AAS Publications Office, PO Box 28130, San Diego, CA 92198.
30. Volkov, I. I. and Yastrebov, V. V., 1990. The improvement of the atmospheric density model using COSMOS satellite orbital evolution, Nabludeniya Isk. Sputn., Astronomical Council of the USSR Acad. No. 86.
31. Cefola, P. J., Proulx, R. J., Nazarenko, A. I., and Yurasov, V. S., 2003. Atmospheric density correction using two line element sets as the observation data. AAS Paper 03-626, AAS 2005-257, AAS Publications Office, PO Box 28130, San Diego, CA 92198.
32. Bowman, B. R., Marcos, F. A., and Kendra, M. J. 2004. A method of computing accurate daily atmospheric density values from satellite drag data. AAS Paper 2004-179, AAS Publications Office, PO Box 28130, San Diego, CA 92198.
33. Torr, D. G., Torr, M. R., Richards, P. G., 1993. Thermospheric airglow emissions: A comparison of measurements from ATLAS-1 and theory, Geophys. Res. Lett., 20, No. 6, pp. 519-522, March 19.
34. Joint Requirements Oversight Council, 2002. NPOESS Integrated Operational Requirements Document II, Joint Chiefs of Staff, Washington, D.C.
35. Ailor, W. H., 2006. Space traffic management: Implementation and implications, Acta Astronautica, in press.
36. Ailor, W. H., Rasky, D. J., and Zell, P., 2005. Pico reentry probes: New tools for reentry testing, (IAC-05-D3.2.07), The Aerospace Corp., El Segundo, CA.
37. Pardini, C., Hanada, T., Krisko, P., Anselmo, L., and Hirayama, H., 2005. Are de-orbiting missions possible using electrodynamic tethers? Task review from the space debris perspective (IAC-05-B6.3.01), ISTI/CNR Pisa, Italy.
38. Patera, R. P., 2004. Managing risk for space object reentry, Space Systems Engineering and Risk Management 2004, Fifth National Symposium, The Aerospace Corporation, El Segundo, CA.
39. Nazarenko, A., 2004. Collision of spacecraft of various shapes with debris particles assessment, AAS Paper 04-180, AAS Publications Office, PO Box 28130, San Diego, CA 92198.
40. Lean, Judith, 2005. Living with a variable sun, Physics Today, 58, 32-38.
41. Gopalswamy, Natchimuthukonar, Mewaldt, Richard, and Torsti, Jarmo, 2006. Solar Eruptions and Energetic Particles, Geophysical Monograph 165, AGU, Washington, D.C.
42. Tsurutani, Bruce, McPherron, Robert, Gonzalez, Walter, Lu, Gang, and Sobral, J. Humberto, 2006. Recurrent Magnetic Storms, Geophysical Monograph 167, AGU, Washington, D. C.
43. Gopalswamy, Nat, 2005. Workshop highlights Progress in Solar-heliospheric physics, EOS, Transactions, AGU, 86, 525-530.
44. Fry, C. D., Dryer, M., Deehr, C. S., Sun, W., Akasofu, S.-I., and Smith. Z., 2003. Forecasting solar-wind structures and shock arrival times using an ensemble of models, J. Geophys. Res. 108 (A2), 1070. doi 10.10/2002JA009474, 2003.

45. McKenna-Lawlor, S., Dryer, M., Kartalev, M. D., Smith, Z., Fry, C. D., Sun, W., Deehr, C. S., Keeskemety, K. and Kudela, K., 2006. Real-time predictions of the arrival at the Earth of flare-generated shocks during solar cycle 23, *J. Geophys. Res.*, in press.
46. Fry, C. D., Detman, T. R., Dryer, M., Smith, Z., Sun, W., Deehr, C. S., Akasofu, S.-I., Wu, C.-C., and McKenna-Lawlor, S., 2006. Real-time solar wind forecasting capabilities and challenges, *J. Atmosph. Solar-Terr. Phys.*, in press.